ETH Eidgenössische Technische Hochschule Zürich
Swiss Federal Institute of Technology Zurich

Seminar for Applied Mathematics SAM

A High-Order Integrator for the Schrödinger Equation with Time-Dependent, Homogeneous Magnetic Field

V. Gradinaru and O. Rietmann

Research Report No. 2018-47
December 2018

Seminar für Angewandte Mathematik
Eidgenössische Technische Hochschule
CH-8092 Zürich
Switzerland

A High-Order Integrator for the Schrödinger Equation with Time-Dependent, Homogeneous Magnetic Field

Vasile Gradinaru, Oliver Rietmann

November 22, 2018

Abstract

We construct a family of numerical methods for the Pauli equation of spinless, charged particles in a time-dependent, homogeneous magnetic field. These methods are described in a general setting comprising systems of multiple particles. The main idea is to split the Pauli equation in three parts, which are solved separately before being merged to a solution of the original problem. In order to decide for a smart way of splitting the Pauli equation, the theory of Lie algebras and their representations is used.

1 The Mathematical Model

Consider a particle of mass $m > 0$ and charge $e \in \mathbb{R}$ living in $\mathbb{R}^d$ subject to a real-valued potential $V(x)$ and a magnetic potential 1-form $A(x,t) = A_k(x,t)\mathrm{d}x^k$, where $x \in \mathbb{R}^d$. We assume the corresponding magnetic field 2-form $\mathrm{d}A$ to be independent of x. Therefore we choose

$$A(x,t) := \frac{1}{2} B_{jk}(t) x^j \mathrm{d}x^k \tag{1.1}$$

where $B(t) = (B_{jk}(t))_{1 \leqslant j,k \leqslant d}$ is a real, skew-symmetric matrix. The corresponding magnetic field 2-form is given by

$$\mathrm{d}A = \sum_{1 \leqslant j < k \leqslant d} B_{jk}(t)\, \mathrm{d}x^j \wedge \mathrm{d}x^k.$$

We introduce for $j, k \in \{1, \ldots, d\}$ the operators [6, Eq (14)], [2, Eq (3.21)]

$$\begin{aligned} p_k &:= -i\hbar\partial_k && \text{(components of linear momentum)} \\ L_{jk} &:= x_j p_k - x_k p_j. && \text{(generalized angular momentum)} \end{aligned}$$

Our system is then described by the Pauli Hamiltonian

$$\begin{aligned} H_P(t) :=& \frac{1}{2m} \sum_{k=1}^{d} \Big(p_k - eA_k(x,t)\Big)^2 + V(x) \\ =& \frac{1}{2m}\Big(\hbar^2(-\Delta) - e \sum_{1 \leqslant j < k \leqslant d} B_{jk}(t) L_{jk} + \frac{e^2}{4} \|B(t)x\|^2_{\mathbb{R}^d}\Big) + V(x). \end{aligned} \tag{1.2}$$

Upon redefining t, x, B and V, we may instead consider the new Hamiltonian

$$H(t) := -\Delta + H_B(t) + V(\,\cdot\,, t) \tag{1.3}$$

on[1] $L^2(\mathbb{R}^d)$, where (now $\hbar = 1$)

$$\begin{aligned} p_k &= -i\partial_k \\ L_{jk} &= x_j p_k - x_k p_j \\ H_B(t) &:= -\sum_{1\leqslant j<k\leqslant d} B_{jk}(t) L_{jk} \end{aligned}$$

with associated Schrödinger equation

$$i\partial_t \psi(\,\cdot\,, t) = H(t)\psi(\,\cdot\,, t), \qquad \psi(\,\cdot\,, 0) = \psi_0. \tag{H}$$

Remark 1.1. *If we choose in* (1.3)

$$V(x,t) = \|B(t)x\|^2_{\mathbb{R}^d} + V(x),$$

we recover (up to scaling) the potential terms in the physical Pauli Hamiltonian (1.2).

The paper is organized as follows: Section 2 describes a numerical method for (H), where each subsection deals with one subproblem. Physical applications and concrete examples of the abstract setting above are in Section 3.

2 The Numerical Method

We split (H) into the three simpler equations:

$$i\partial_t \psi(\,\cdot\,, t) = -\Delta\psi(\,\cdot\,, t) \tag{K}$$
$$i\partial_t \psi(\,\cdot\,, t) = H_B(t)\psi(\,\cdot\,, t) \tag{M}$$
$$i\partial_t \psi(\,\cdot\,, t) = V(\,\cdot\,, t)\psi(\,\cdot\,, t) \tag{P}$$

The main steps of our method are:

1. Solve the kinetic equation (K) using Fourier transform (FFT).
2. Reduce the magnetic equation (M) to the linear ODE[1]

   $$\frac{\mathrm{d}}{\mathrm{d}t} y(t) = B(t)\, y(t), \tag{B}$$

   where $y : \mathbb{R} \to \mathbb{R}^d$. This is achieved using a Lie algebra isomorphism relating $B(t)$ and $H_B(t)$. We then use Magnus expansion to solve (B).
3. Using that $-\Delta$ and $H_B(t)$ (and thus their flow maps) commute, combine the previous solutions to a solution of

   $$i\partial_t \psi = (-\Delta + H_B(t))\psi. \tag{K+M}$$

[1] We write $L^2(\mathbb{R}^d) := L^2(\mathbb{R}^d; \mathbb{C})$ for the **complex-valued**, square-integrable functions.
[1] After multiplication by i on both sides, (B) becomes a Schrödinger equation with Hamiltonian $iB(t)$.

4. Solve the potential equation (P) using pointwise multiplication by $e^{-i\int_{t_0}^{t} V(\,\cdot\,,s)\mathrm{d}s}$.

5. A splitting scheme merges the solutions from steps 3 and 4 to a solution of (H).

In the rest of this section, we will discuss the steps 2, 3 and 5 in more detail. The following notation will be useful in this regard: Given a Hamiltonian $\tilde{H}(t)$ we denote by $\Phi_{\tilde{H}}(t,t_0)$ the unitary flow associated to the time-dependent Schrödinger equation

$$i\partial_t\psi(\,\cdot\,,t) = \tilde{H}(t)\psi(\,\cdot\,,t), \qquad \psi_0 = \psi(\,\cdot\,,0),$$

i.e. $\Phi_{\tilde{H}}(t,t_0)\psi_0$ satisfies

$$\frac{\mathrm{d}}{\mathrm{d}t}\Phi_{\tilde{H}}(t,t_0) = -i\tilde{H}(t)\Phi_{\tilde{H}}(t,t_0). \tag{2.1}$$

2.1 Step 2: Solving Equation (M)

The equations (B) and (M) are closely related by the unitary representation

$$\rho : \mathrm{SO}(d) \longrightarrow \mathrm{U}(L^2(\mathbb{R}^d))$$

defined as the map satisfying

$$(\rho(R)\psi)(x) = \psi(R^{-1}x) \tag{2.2}$$

for all $R \in \mathrm{SO}(d), \psi \in L^2(\mathbb{R}^d)$ and all $x \in \mathbb{R}^d$. We investigate this relation by considering the Lie algebra

$$\mathfrak{so}(d) := \{\Omega \in \mathbb{R}^{d\times d} \mid \Omega^{\mathrm{T}} = -\Omega\}$$

of $\mathrm{SO}(d)$. Note that $B(t) \in \mathfrak{so}(d)$ for all $t \in \mathbb{R}$. The derivative of ρ is the Lie algebra isomorphism (compare [2, Eq (2.14)] and [2, Eq (3.28)])

$$\rho_* : \mathfrak{so}(d) \longrightarrow \mathfrak{l}(L^2(\mathbb{R}^d)),\ \Omega \longmapsto -iH_\Omega,$$

where

$$\mathfrak{l}(L^2(\mathbb{R}^d)) := \mathrm{span}_{\mathbb{R}}\{iL_{jk} \,|\, 1 \leqslant j < k \leqslant d\}$$

is endowed with the usual commutator. Then the following diagram commutes:

$$\begin{array}{ccc} \mathfrak{so}(d) & \xrightarrow{\ \rho_*\ } & \mathfrak{l}(L^2(\mathbb{R}^d)) \\ \Big\downarrow{\scriptstyle \exp} & & \Big\downarrow{\scriptstyle \exp} \\ \mathrm{SO}(d) & \xrightarrow[\ \rho\ ]{} & \mathrm{U}(L^2(\mathbb{R}^d)) \end{array}$$

Moreover, [8, Thm X.69] yields existence of a flow map $U(t,t_0) \in \mathrm{SO}(d)$ solving (B), i.e.

$$\frac{\mathrm{d}}{\mathrm{d}t}U(t,t_0) = B(t)U(t,t_0), \qquad U(t_0,t_0) = \mathrm{id}\,. \tag{2.3}$$

This discussion motivates the following.

Lemma 2.1. *The flow map $U(t,t_0)$ of* (B) *gives rise to a flow map of* (M) *by*

$$\Phi_{H_B}(t,t_0) = \rho(U(t,t_0))$$

for all $t, t_0 \in \mathbb{R}$.

Proof. Observe that

$$-iH_B(t) = \sum_{j,k=1}^{d} B_{jk}(t) x_j \partial_k. \tag{2.4}$$

and fix $t, t_0 \in \mathbb{R}$. For all $j, k \in \{1, \dots, d\}$ and all $x \in \mathbb{R}^d$, we have

$$x_j \partial_k \psi_0(U^{-1}(t,t_0)x) = \mathrm{d}\psi_0\big|_{U^{-1}(t,t_0)x} \cdot x_j \partial_k U^{-1}(t,t_0)x = \mathrm{d}\psi_0\big|_{U^{-1}(t,t_0)x} \cdot U^{-1}(t,t_0) x_j \partial_k x.$$

Hence by (2.4) and linearity

$$-iH_B(t)\,\psi_0(U^{-1}(t,t_0)x) = \mathrm{d}\psi_0\big|_{U^{-1}(t,t_0)x} \cdot U^{-1}(t,t_0)(-iH_B(t)x).$$

Anti-symmetry of $B(t)$ and (2.4) yield similarly for all $x \in \mathbb{R}^d$

$$-iH_B(t)x = -B(t)x.$$

We take the transpose on both sides of (2.3) and use anti-symmetry of $B(t)$ again in order to get

$$\frac{\mathrm{d}}{\mathrm{d}t} U^{-1}(t,t_0) = (-1)U^{-1}(t,t_0)B(t).$$

Fix some initial data $\psi_0 \in L^2(\mathbb{R})$. Using the last three equations, we compute

$$\begin{aligned} -iH_B(t)\,\psi_0(U^{-1}(t,t_0)x) &= \mathrm{d}\psi_0\big|_{U^{-1}(t,t_0)x} \cdot U^{-1}(t,t_0)(-iH_B(t)x) \\ &= \mathrm{d}\psi_0\big|_{U^{-1}(t,t_0)x} \cdot (-1)U^{-1}(t,t_0)B(t)x \\ &= \mathrm{d}\psi_0\big|_{U^{-1}(t,t_0)x} \cdot \frac{\mathrm{d}}{\mathrm{d}t} U^{-1}(t,t_0)x \\ &= \frac{\mathrm{d}}{\mathrm{d}t} \psi_0(U^{-1}(t,t_0)x). \end{aligned}$$

Hence $\rho(U(t,t_0))$ is a flow map for (M). □

2.2 Step 2: Solving Equation (B) by Magnus Expansion

We approximate the exact flow $U(t,t_0) \in \mathrm{SO}(d)$ of (B) by a Magnus expansion (see [7] or [4, Ch IV.7] for details), i.e.

$$U(t,t_0) \approx U_n(t,t_0) := e^{\Omega^{[n]}(t,t_0)}, \qquad \Omega^{[n]}(t,t_0) := \sum_{m=1}^{n} \Omega_m(t,t_0), \tag{2.5}$$

for some $\Omega_m(t,t_0) \in \mathfrak{so}(d)$ and the first two terms of the truncated series are

$$\Omega_1(t,t_0) = \int_{t_0}^{t} B(s_1)\mathrm{d}s_1, \qquad \Omega_2(t,t_0) = \frac{1}{2}\int_{t_0}^{t}\int_{t_0}^{s_1} \big[B(s_1), B(s_2)\big]\mathrm{d}s_2\mathrm{d}s_1.$$

The Magnus expansion yields a unitary approximation of $\Phi_{H_B}(t,t_0) = \rho(U(t,t_0))$ as stated in the next lemma.

Lemma 2.2. *For all $t, t_0 \in \mathbb{R}$ and all $n \in \mathbb{N}$, we have*

(i) $U_n(t,t_0) \in \mathrm{SO}(d)$ and

(ii) $\rho(U_n(t,t_0))$ is a unitary map on $L^2(\mathbb{R}^d)$.

Proof. Part (i) holds since the matrix exponential on a Lie algebra maps to its Lie group. Moreover, (i) implies (ii) by means of the substitution $y := U_n^{-1}(t,t_0)x$ in the integral of the inner product on $L^2(\mathbb{R}^d)$. □

2.3 Step 3: Solving Equation (K+M)

The following lemma shows that we can switch the flows and hence the internal steps in our algorithm in a convenient way. It also justifies the treatment of $-\Delta$ and H_B together in one step.

Lemma 2.3. *Fix any $t, t_0 \in \mathbb{R}$. Then*

(i) for all $R \in \mathrm{SO}(d)$ the operators $\rho(R)$ and $\Phi_{-\Delta}(t, t_0)$ commute and

(ii) we have $\Phi_{-\Delta+H_B}(t, t_0) = \Phi_{H_B}(t, t_0)\,\Phi_{-\Delta}(t, t_0) = \Phi_{-\Delta}(t, t_0)\,\Phi_{H_B}(t, t_0)$.

Proof. Fix any $R \in \mathrm{SO}(d)$. Note that $\rho(R)$ commutes with the Fourier transform $\mathcal{F}$ and that $\mathbb{R}^d \to \mathbb{C},\ k \mapsto e^{-i(t-t_0)k^2}$ is rotation invariant. Hence

$$\begin{aligned}\rho(R)e^{-i(t-t_0)(-\Delta)} &= \rho(R)\mathcal{F}^{-1}e^{-i(t-t_0)k^2}\mathcal{F} \\ &= \mathcal{F}^{-1}e^{-i(t-t_0)k^2}\mathcal{F}\rho(R) \\ &= e^{-i(t-t_0)(-\Delta)}\rho(R).\end{aligned}$$

This proves (i), which in turn proves the second equality in (ii) by Lemma 2.1. It remains to show that the first equality also holds:

$$\begin{aligned}\frac{\mathrm{d}}{\mathrm{d}t}\big(\Phi_{H_B}(t,t_0)\Phi_{-\Delta}(t,t_0)\big) &= \dot{\Phi}_{H_B}(t,t_0)\Phi_{-\Delta}(t,t_0) + \Phi_{H_B}(t,t_0)\dot{\Phi}_{-\Delta}(t,t_0) \\ &\overset{(2.1)}{=} -iH_B(t)\Phi_{H_B}(t,t_0)\Phi_{-\Delta}(t,t_0) - i\Phi_{H_B}(t,t_0)(-\Delta)\Phi_{-\Delta}(t,t_0) \\ &= -i\big(-\Delta + H_B(t)\big)\Phi_{H_B}(t,t_0)\Phi_{-\Delta}(t,t_0),\end{aligned}$$

where we used rotation invariance of the Laplacian to swap $-\Delta$ and $\Phi_{H_B}(t, t_0)$. It follows that $\Phi_{H_B}(t, t_0)\Phi_{-\Delta}(t, t_0)$ solves (2.1) for $\tilde{H} = -\Delta + H_B$, which concludes the proof. □

2.4 Step 5: Solving Equation (H) by Splitting

Let $U(t, t_0)$ denote the flow map of (B) and ρ the left-regular representation defined in (2.2). We construct an approximation of the solution of the time-dependent Schrödinger Equation (H) associated with the full Hamiltonian

$$H(t) = -\Delta + H_B(t) + V(\,\cdot\,, t) \tag{1.3}$$

by a splitting with coefficients $(a_i, b_i)_{i\in\{1,\dots,n\}}$. We start with a few notations. Fix times $t_0 < t$ and introduce for $i \in \{0, \dots, n\}$ the time grids

$$t_i = t_0 + (t - t_0)\sum_{j=1}^{i} b_j \quad \text{and} \quad s_i = t_0 + (t - t_0)\sum_{j=1}^{i} a_j \tag{2.6}$$

and for any two Hamiltonians H_1 and H_2 write[2]

$$(\Phi_{H_2} \overset{(a,b)}{\circ} \Phi_{H_1})(t, t_0) := \prod_{i=0}^{n-1} \Phi_{H_2}(t_{i+1}, t_i)\Phi_{H_1}(s_{i+1}, s_i).$$

[2]The order of the product is “lowest index first”: $\prod_{i=1}^{n} A_i := A_n \cdots A_1$

Our splitting scheme for (H) then reads

$$\Phi_H(t,t_0) \approx (\Phi_{-\Delta+H_B} \overset{(a,b)}{\circ} \Phi_V)(t,t_0) = \prod_{i=0}^{n-1} \Phi_{-\Delta}(t_{i+1},t_i)\Phi_{H_B}(t_{i+1},t_i)\Phi_V(s_{i+1},s_i)$$

where we used part (ii) of Lemma 2.3. The equality

$$\rho(R)(f\cdot\psi) = (\rho(R)f)\cdot(\rho(R)\psi)$$

holds for all[3] $\psi \in L^2(\mathbb{R}^d)$, $f \in L^\infty(\mathbb{R}^d)$ and all $R \in \mathrm{SO}(d)$. We apply it to the special choice $R = U(t,t')$ and $f(\,\cdot\,) = \Phi_V(s,s') = e^{-i\int_{s'}^{s} V(\,\cdot\,,\tilde{s})\mathrm{d}\tilde{s}}$. Lemma 2.1 yields then

$$\Phi_{H_B}(t,t')\Phi_V(s,s') = \Phi_{\rho(U(t,t'))V}(s,s')\Phi_{H_B}(t,t') \tag{2.7}$$

for all $t,t',s,s' \in \mathbb{R}$. This is crucial for proving Lemma 2.4 below, which provides an expression for $(\Phi_{-\Delta+H_B} \overset{(a,b)}{\circ} \Phi_V)(t,t_0)$ in terms of rotated potentials and a single rotation of the initial data.

Lemma 2.4. *For splitting coefficients $(a_i,b_i)_{i\in\{1,\dots,n\}}$ and times $s_0,\dots,s_n,t_0,\dots,t_n,t$ as in* (2.6)*, we have*

$$(\Phi_{-\Delta+H_B} \overset{(a,b)}{\circ} \Phi_V)(t,t_0) = \left(\prod_{i=0}^{n-1} \Phi_{-\Delta}(t_{i+1},t_i)\Phi_{\rho(U(t_n,t_i))V}(s_{i+1},s_i)\right)\Phi_{H_B}(t_n,t_0).$$

Proof. We proceed by induction on n. For $n=1$, the assertion follows immediately from (2.7). Suppose now that the formula holds for any set of coefficients of length $n-1$. Using this hypothesis on the last $n-1$ factors and Lemma 2.3, we obtain

$$\begin{aligned}(\Phi_{-\Delta+H_B} \overset{(a,b)}{\circ} \Phi_V)(t,t_0) &= \left(\prod_{i=1}^{n-1} \Phi_{-\Delta}(t_{i+1},t_i)\Phi_{\rho(U(t_n,t_i))V}(s_{i+1},s_i)\right)\Phi_{H_B}(t_n,t_1)\times\cdots\\ &\cdots\times\Phi_{-\Delta}(t_1,t_0)\Phi_{H_B}(t_1,t_0)\Phi_V(s_1,s_0)\\ &= \left(\prod_{i=1}^{n-1} \Phi_{-\Delta}(t_{i+1},t_i)\Phi_{\rho(U(t_{i+1},t_i))V}(s_{i+1},s_i)\right)\times\cdots\\ &\cdots\times\Phi_{-\Delta}(t_1,t_0)\Phi_{H_B}(t_n,t_0)\Phi_V(s_1,s_0)\\ &= \left(\prod_{i=1}^{n-1} \Phi_{-\Delta}(t_{i+1},t_i)\Phi_{\rho(U(t_n,t_i))V}(s_{i+1},s_i)\right)\times\cdots\\ &\cdots\times\Phi_{-\Delta}(t_1,t_0)\Phi_{\rho(U(t_n,t_0))V}(s_1,s_0)\Phi_{H_B}(t_n,t_0)\end{aligned}$$

which is exactly the claim for n factors. □

We have only treated a single time-step $[t_0,t]$ so far. But using Lemma 2.4 and (2.7) we can generalize the idea to N steps of length $h := t-t_0$ as follows:

$$\Phi_H(t_0+Nh,t_0) \approx \left(\prod_{j=0}^{N-1}\prod_{i=0}^{n-1} \Phi_{-\Delta}(t_{i+1},t_i)\Phi_{\rho(U(t_0+Nh,t_i+jh))V}(s_{i+1}+jh,s_i+jh)\right)\Phi_{H_B}(t_0+Nh,t_0). \tag{2.8}$$

Algorithm 1 provides a pseudo-code for efficient computing of the right-hand side in (2.8). It only remains to approximate the flow $U(\,\cdot\,,\,\cdot\,)$, for instance by a Magnus expansion as discussed in Lemma 2.2.

[3]Even if $f \notin L^2(\mathbb{R}^d)$ we still define $\rho(R)f$ as in (2.2).

Remark 2.1. *If for all $t \in \mathbb{R}$ the potential $V(\,\cdot\,, t)$ is spherically symmetric, i.e.*

$$\forall R \in SO(d) : \rho(R)V(\,\cdot\,, t) = V(\,\cdot\,, t),$$

then we may replace $\rho(U(t_0 + Nh, t_i + jh))V = V$ in (2.8).

Algorithm 1 Compute the RHS of (2.8)

Input: first time step $[t_0, t]$; number of time steps N; meshgrid X; initial wave function ψ_0 at time t_0; potential V; splitting coefficients $(a_i, b_i)_{i\in\{1,\dots,n\}}$; flow maps $\Phi_{-\Delta}, \Phi_V$ and U corresponding to (K),(P) and (B);

Output: Y is the solution at time $(t-t_0)\cdot N+t_0$ evaluated on X;

$h := t - t_0$
$t_a := t_0$
$t_b := t_0$
$R := U(t_0 + N \cdot h, t_0)$
$Y := \psi_0 \circ R^{-1}(X)$ $\{= (\rho(R)\psi_0)(X)\}$
for $j = 0$ to $N - 1$ **do**
    for $i = 1$ to n **do**
        $\tilde{V} := V \circ R^{-1}$ $\{= \rho(R)V\}$
        $Y = \Phi_{\tilde{V}}(t_a + a_i \cdot h, t_a)Y$
        $R = R \cdot U^{-1}(t_b + b_i \cdot h, t_b)$
        $Y = \Phi_{-\Delta}(t_b + b_i \cdot h, t_b)Y$
        $t_a = t_a + a_i \cdot h$
        $t_b = t_b + b_i \cdot h$
    end for
end for
return Y

---

3 Examples

The Pauli Hamiltonian (1.2) (and thus also its abstract version (1.3)) contains many physically relevant cases. In order to investigate them, it is convenient to introduce the notation

$$\Omega(\vec{B}) := \begin{pmatrix} 0 & -B_3 & B_2 \\ B_3 & 0 & -B_1 \\ -B_2 & B_1 & 0 \end{pmatrix}, \qquad \vec{B} = \begin{pmatrix} B_1 \\ B_2 \\ B_3 \end{pmatrix} \in \mathbb{R}^3.$$

Example 3.1 (N particles in three dimensions)**.** *Consider a system of N particles of mass $m > 0$ and charge $e \in \mathbb{R}$ where $n \in \{1, \dots, N\}$, subject to a potential $V(\vec{x}_1, \dots, \vec{x}_N)$ and a homogeneous magnetic field $\vec{B}(t)$. This system is modeled by the Pauli Hamiltonian*

$$H_N = \frac{1}{2m} \sum_{n=1}^{N} \left(\vec{p}_n - e\vec{A}(\vec{x}_n, t)\right)^2 + V(\vec{x}_1, \dots, \vec{x}_N)$$

where $\vec{p}_n := -i\hbar\vec{\nabla}_n$ and the vector potential is given by

$$\vec{A}(\vec{x}, t) := \frac{1}{2}\vec{B}(t) \times \vec{x}.$$

By choosing $d = 3N$ *and*

$$B(t) = \operatorname{diag}\big(\Omega(-\vec{B}(t)), \dots, \Omega(-\vec{B}(t))\big)$$

in (1.1) *we can obtain this as special case of* (1.2)*.*

Example 3.2 (N particles in two dimensions)**.** *The setting of Example 3.1 can be adapted to N particles moving only in the (x, y)-plane. The magnetic field can be assumed perpendicular to the plane of motion, say $\vec{B}(t) = (0, 0, B_3(t))^{\mathrm{T}}$. Thus we have to choose $d = 2N$ and*

$$B(t) = \operatorname{diag}\left(\begin{pmatrix} 0 & B_3 \\ -B_3 & 0 \end{pmatrix}, \dots, \begin{pmatrix} 0 & B_3 \\ -B_3 & 0 \end{pmatrix} \right)$$

in (1.1) *to retrieve this system as a special case of* (1.2)*.*

Remark 3.1. *By Remark 1.1, we can recover* (1.2) *(up to scaling) from* (1.3) *by choosing*

$$V(x, t) = \|B(t)x\|^2_{\mathbb{R}^d} + V(x).$$

The integral in the associated unitary flow

$$\Phi_V(t, t_0) = \exp\left(-i \int_{t_0}^{t} V(x, s)\mathrm{d}s \right)$$

can be computed independently of $x \in \mathbb{R}^d$ (and thus efficiently) since

$$\begin{aligned} \int_{t_0}^{t} V(x, s)\mathrm{d}s &= \int_{t_0}^{t} \big\langle B(s)x, B(s)x \big\rangle_{\mathbb{R}^d} \mathrm{d}s + (t - t_0)V(x) \\ &= \left\langle x, \left(-\int_{t_0}^{t} B^2(s)\mathrm{d}s \right) x \right\rangle_{\mathbb{R}^d} + (t - t_0)V(x), \end{aligned}$$

where we used the skew-symmetry of B in the last step.

Remark 3.2. *The assumption that all particles share the same mass and charge is only for simplicity. Redefining the coordinates x, t as well as B and V allows us to reduce the general case to one of the examples above.*

Remark 3.3. *Note that the block form of $B(t)$ in the previous examples simplifies the computation of the exponential in the Magnus expansion* (2.5)*: In the notation of* (2.5)*, the matrices $\Omega_m(t, t_0)$ inherit the block form. Similarly, $\Omega^{[n]}(t, t_0)$ and $U_n(t, t_0) = e^{\Omega^{[n]}(t, t_0)}$ become block-diagonal.*

3.1 Order of Convergence (Harmonic Potential)

We now examine the order of convergence of our method for different splittings (see step 5). Therefore, we solve (H) for $t \in [0, 2\pi]$ with magnetic field

$$B(t) = \Omega(-\vec{B}(t)), \qquad \vec{B}(t) = \frac{\cos(t)}{\sqrt{3}} \begin{pmatrix} 1 \\ 1 \\ 1 \end{pmatrix}.$$

The potential in (1.3) is chosen as[4]

$$V(\vec{x},t) = x_1^2 + x_2^2 + x_3^2.$$

The initial data at time $t = 0$ shall be the Gaussian

$$\psi_0(\vec{x}) = \frac{1}{(2\pi\sigma^2)^{\frac{3}{4}}} \exp\left(-\frac{(\vec{x}-\vec{\mu})^2}{4\sigma^2} + 2ix_1 \right), \qquad \vec{\mu} := \begin{pmatrix}1\\1\\1\end{pmatrix}, \ \sigma^2 := \frac{1}{2} \tag{3.1}$$

of L^2-norm one. This setting admits periodic solutions of period 2π. In particular, the solution $\psi(\vec{x},t)$ to this IVP satisfies $\psi_0(\vec{x}) = \psi(\vec{x},2\pi)$ for all $\vec{x} \in \mathbb{R}$. The initial data will thus serve as reference solution for the convergence plots in Figure 1. They indicate that the order of our method is equal to the order of the underlying splitting scheme.

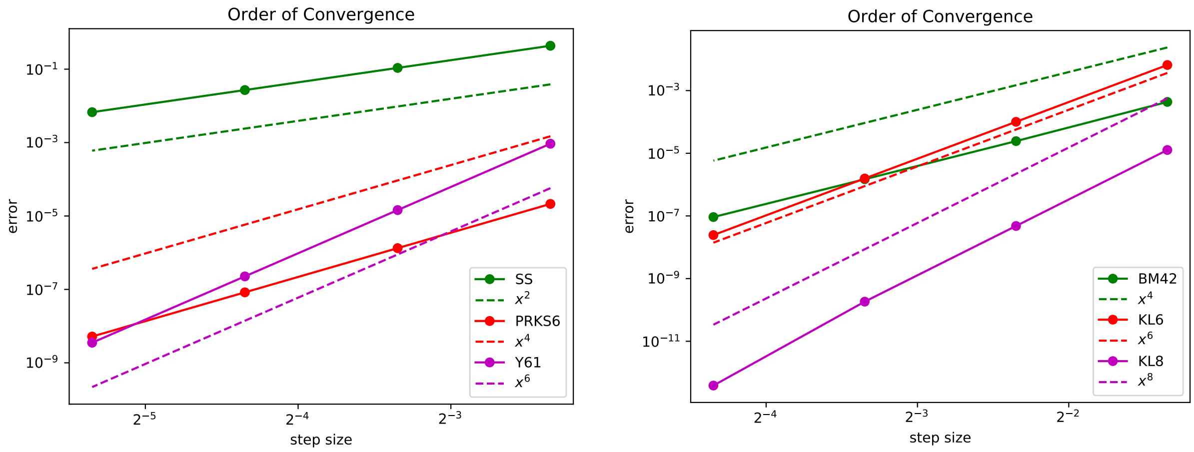

Figure 1: Order of convergence using different splittings. See Table 1 for the legend.

Method	Order	Author(s)	Reference(s)
SS	2	Strang	[9], [3]: Page 42, Eq. 5.3
PRKS6	4	Blanes/Moan	[1]: Page 318, Table 2, 'S6'
BM42	4	Blanes/Moan	[1]: Page 318, Table 3, 'SRKNb6'
Y61	6	Yoshida	[10], [3]: Page 144, Eq. 3.11
KL6	6	Kahan/Li	[5], [3]: Page 144, Eq. 3.12
KL8	8	Kahan/Li	[5], [3]: Page 145, Eq. 3.14

Table 1: Legend for the splittings in Figure 1.

3.2 Order of Convergence (Mexican Hat Potential)

Now we consider the more involved example of a Mexican hat potential

$$V(\vec{x}) = \frac{1}{32}\|\vec{x}\|_{\mathbb{R}^3}^4 - x_1^2 - \frac{3}{2}x_2^2 - 2x_3^2.$$

[4]This is *not* a special case of the Pauli Hamiltonian (1.2) since $V(\vec{x},t)$ is independent of the magnetic field. Compare to Remark 1.1.

The magnetic field is given by

$$B(t) = \Omega(-\vec{B}(t)), \qquad \vec{B}(t) = \frac{1}{\sqrt{3}} \begin{pmatrix} \cos(t) \\ \sin(t) \\ 1 \end{pmatrix}.$$

Thus we arrive at the time-dependent potential (see Remark 1.1)

$$V(\vec{x}, t) = \|B(t)\vec{x}\|_{\mathbb{R}^3}^2 + V(\vec{x}).$$

We solve the corresponding time-dependent Schrödinger equation (H) on $t \in [0, 2\pi]$ using different splitting schemes. As before, (3.1) serves as initial data. The accurate KL8 splitting with time steps of size $h = 2\pi \cdot 2^{-8}$ provides the reference solution for the results in Figure 2.

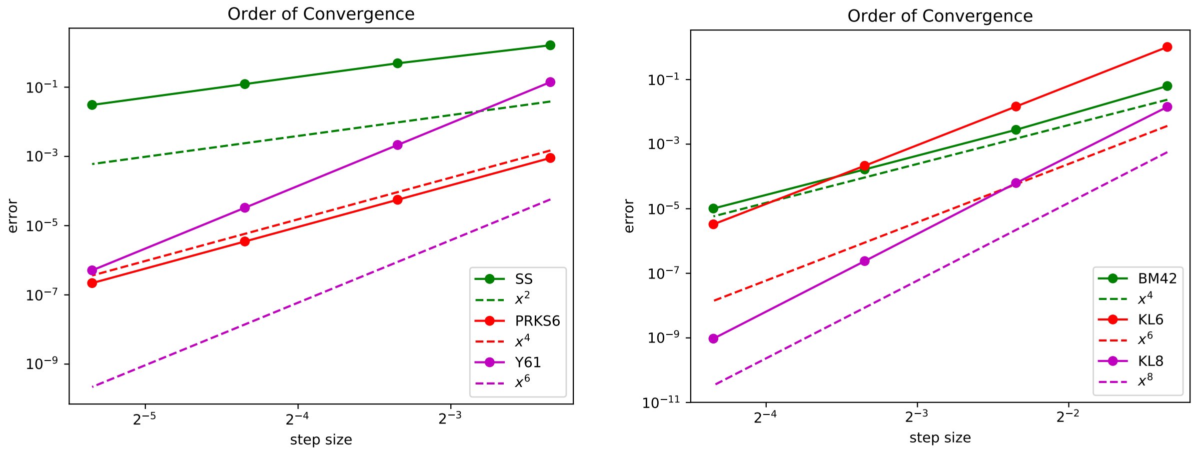

Figure 2: Order of convergence using different splittings. See Table 1 for the legend.

3.3 Norm and Energy Conservation (Morse Potential)

In this example we focus on the conservation of the L^2-norm and of the energy. The latter is conserved if the Hamiltonian is constant in time. We thus consider a modification of the Example 3.2 to the threefold Morse potential (see Figure 3)

$$V(x) = 16\left(1 - \exp\left(-\frac{\|x\|_{\mathbb{R}^2}^2}{32}\left(1 - \cos(3\arctan2(x_2, x_1))\right)^2\right)\right)^2$$

and the constant magnetic field

$$B(t) = \frac{1}{2}\begin{pmatrix} 0 & -1 \\ 1 & 0 \end{pmatrix}$$

perpendicular to the plane of motion. The overall potential is hence now time-independent (see Remark 1.1)

$$V(x, t) = \|B(t)x\|_{\mathbb{R}^2}^2 + V(x) = \frac{1}{4}\|x\|_{\mathbb{R}^2}^2 + V(x)$$

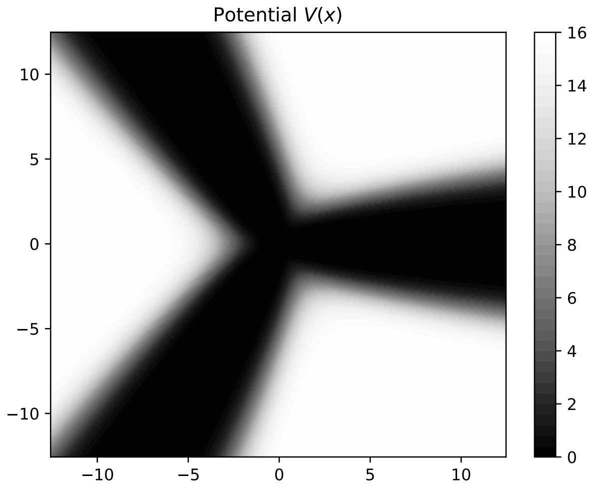

Figure 3: The threefold Morse potential. We expect a high probability of finding the particle within the back region, which is confirmed by Figure 5 below.

Finally, we take the Gaussian initial data

$$\psi_0(x) = \frac{1}{\sqrt{2\pi\sigma^2}} \exp\left(- \frac{(x-\mu)^2}{4\sigma^2} + 2ix_1 \right), \qquad \mu := \begin{pmatrix} 1 \\ 1 \end{pmatrix}, \ \sigma^2 := \frac{1}{2}$$

of L^2-norm one. Write $\psi(t) = \psi(\,\cdot\,, t)$ and denote by $\langle \cdot\,, \cdot \rangle_{L^2}$ the inner product on $L^2(\mathbb{R}^d)$. We consider the energies

$$\begin{aligned}
E_{\text{kin}}(t) &:= \langle \psi(t), -\Delta\psi(t) \rangle_{L^2} && \text{(kinetic energy)} \\
E_{\text{mag}}(t) &:= \langle \psi(t), (H_{-B}(t) + \|B(t)x\|^2_{\mathbb{R}^d})\psi(t) \rangle_{L^2} && \text{(magetic energy)} \\
E_{\text{pot}}(t) &:= \langle \psi(t), V(x)\psi(t) \rangle_{L^2} && \text{(potential energy)} \\
E_{\text{tot}}(t) &:= E_{\text{kin}}(t) + E_{\text{mag}}(t) + E_{\text{pot}}(t). && \text{(total energy)}
\end{aligned}$$

for $d = 2$. Figure 4 indicates that the total energy is preserved, although its components exhibit non-trivial behavior. Moreover, the L^2-norm is approximately constant as well.

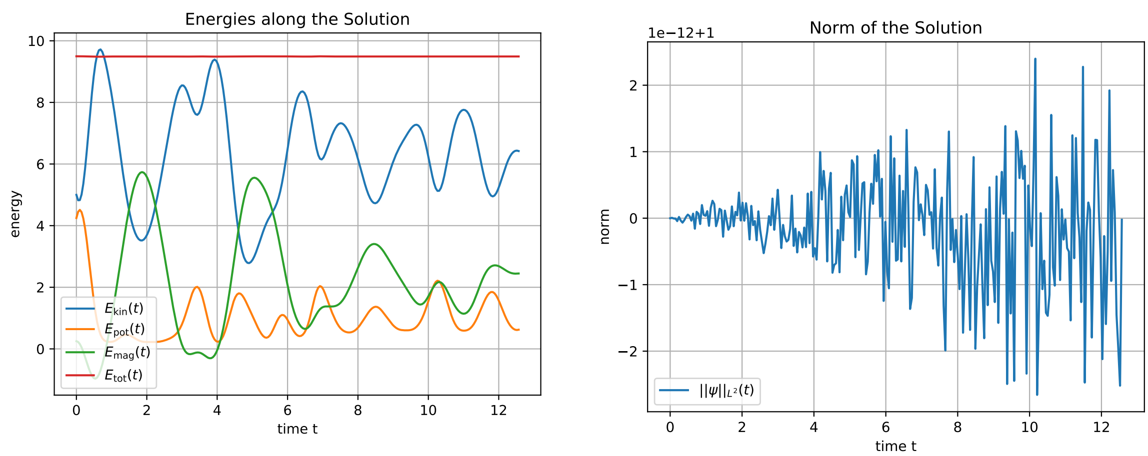

Figure 4: Energies and L^2-norm along the solution in the setting above.

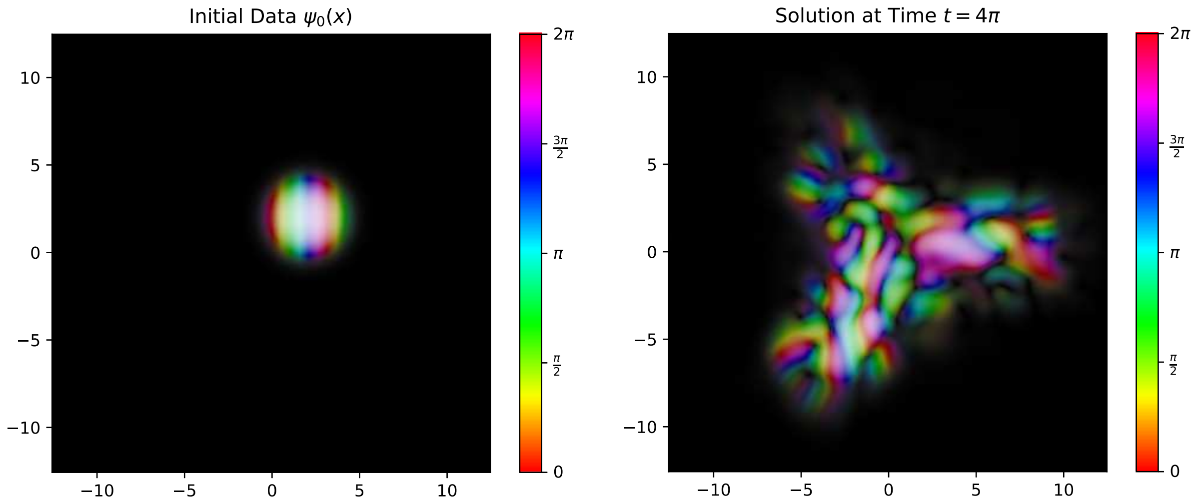

Figure 5: Initial data and solution in the setting above. A complex valued wave-function ϕ is plotted as follows: The color at x encodes the phase of $\phi(x)$, while we darken the pixel according to the modulus $|\phi(x)|$. A black pixel indicates a vanishing wave function at this point and the larger the value of $|\phi(x)|$, the brighter the pixel at x.

References

[1] Sergio Blanes and Per Christian Moan. Practical symplectic partitioned Runge–Kutta and Runge–Kutta–Nyström methods. *Journal of Computational and Applied Mathematics*, 142(2):313–330, 2002.

[2] Shi-Hai Dong. *Wave equations in higher dimensions*. Springer, Dordrecht, 2011.

[3] Ernst Hairer, Christian Lubich, and Gerhard Wanner. *Geometric numerical integration: Structure-preserving algorithms for ordinary differential equations*, volume 31 of *Springer series in computational mathematics*. Springer, Berlin, second edition, 2010.

[4] Brian C. Hall. *Quantum theory for mathematicians*, volume 267 of *Graduate texts in mathematics*. Springer, New York, 2013.

[5] William Kahan and Ren-Cang Li. Composition constants for raising the orders of unconventional schemes for ordinary differential equations. *Mathematics of Computation*, 66:1089–1099, 1997.

[6] James D. Louck. Generalized orbital angular momentum and the n-fold degenerate quantum-mechanical oscillator: Part II. The n-fold degenerate oscillator. *Journal of Molecular Spectroscopy*, 4(1):298–333, 1960.

[7] Wilhelm Magnus. On the exponential solution of differential equations for a linear operator. *Communications on Pure and Applied Mathematics*, 7(4):649–673, 1954.

[8] Barry Simon and Michael Reed. *Fourier analysis, self-adjointness*, volume 2 of *Methods of modern mathematical physics*. Academic Press, Boston, 1975.

[9] Gilbert Strang. On the construction and comparison of difference schemes. *SIAM Journal on Numerical Analysis*, 5:506–517, 1968.

[10] Haruo Yoshida. Construction of higher order symplectic integrators. *Physics Letters A*, 150(5):262–268, 1990.